BMC Medicine

RESEARCH

Open Access

Interactive effect of air pollution and genetic risk of depression on processing speed by resting-state functional connectivity of occipitoparietal network

Yuyanan Zhang[1], Zhe Lu[1*], Yaoyao Sun[1], Liangkun Guo[1], Xiao Zhang[1], Yundan Liao[1], Zhewei Kang[1], Xiaoyang Feng[1], Guorui Zhao[1], Junyuan Sun[1], Yang Yang[1], Hao Yan[1], Dai Zhang[1] and Weihua Yue[1,2,3,4*]

Abstract

Background Air pollution, a reversible environmental factor, was significantly associated with the cognitive domains that are impaired in major depressive disorder (MDD), notably processing speed. Limited evidence explores the interactive effect of air pollution and the genetic risk of depression on cognition. This cross-sectional study aims to extend the research by specifically examining how this interaction influences depression-related cognitive impairment and resting-state brain function.

Methods Eligible participants were 497 healthy adult volunteers (48.7% males, mean age 24.5) living in Beijing for at least 1 year and exposed to relatively high air pollution from the local community controlling for socioeconomic and genomic. Six months' ambient air pollution exposures were assessed based on residential addresses using monthly averages of fine particulate matter with a diameter of less than or equal to 2.5 μm ($PM_{2.5}$). A cross-sectional analysis was conducted using functional magnetic resonance imaging (fMRI) and cognitive performance assessments. The polygenic risk score (PRS) of MDD was used to estimate genetic susceptibility.

Results Using a general linear model and partial least square regression, we observed a negative association between resting-state local connectivity in precuneus and PRS-by-$PM_{2.5}$ interactive effect ($P_{FWE}=0.028$), indicating that $PM_{2.5}$ exposure reduced the spontaneous activity in precuneus in individuals at high genetic risk for MDD. DNA methylation and gene expression of the *SLC30A3* gene, responsible for maintaining zinc-glutamate homeostasis, was suggestively associated with this local connectivity. For the global functional connectivity, the polygenic risk for MDD augmented the neural impact of $PM_{2.5}$ exposure, especially in the frontal-parietal and frontal-limbic regions of the default mode network ($P_{FDR}<0.05$). In those genetically predisposed to MDD, increased $PM_{2.5}$ exposure positively correlated with resting-state functional connectivity between the left angular gyrus and left cuneus gyrus. This connectivity was negatively associated with processing speed.

*Correspondence:
Zhe Lu
luzhe@bjmu.edu.cn
Weihua Yue
dryue@bjmu.edu.cn
Full list of author information is available at the end of the article

Conclusions Our cross-sectional study suggests that air pollution may be associated with an increased likelihood of cognitive impairment in individuals genetically predisposed to depression, potentially through alterations in the resting-state function of the occipitoparietal and default mode network.

Keywords Air pollution, Major depressive disorder, Resting-state brain function, Cognition, Gene-environment interaction

Background

Ambient (outdoor) air pollution has been estimated to cause 4.2 million premature deaths worldwide per year in both cities and rural areas [1]. Beyond the alarming statistics of premature deaths, emerging research has shed light on the intricate interplay between air pollution and mental health outcomes, notably depression [2–4]. Experimental studies with mice exposed to air pollution nanoparticles have provided evidence of cognitive impairment, depressive-like behaviors, and hippocampal microglia activation [5]. Fine particulate matter with a diameter of less than or equal to 2.5 μm ($PM_{2.5}$) has been consistently identified as a major air pollutant that significantly impacts cognitive function, particularly those commonly impaired in depression, such as processing speed and executive/working memory [6], and thus becomes the primary focus. $PM_{2.5}$ could directly penetrate the central nervous system, potentially rendering the developing brain more susceptible to toxic effects and leading to structural and functional alterations [7], ultimately increasing the risks of depression and its related cognitive impairment [8].

Recent evidence suggests that individuals with a higher genetic risk are more susceptible to developing depression when exposed to elevated levels of air pollution [3]. However, the interactive effect of air pollution and the genetic risk of major depressive disorder (MDD) on cognitive impairment has not been extensively explored. It is noteworthy to extend this line of research by specifically examining how this interaction influences depression-related cognitive impairment, focusing on processing speed and executive/working memory. Polygenic risk score (PRS) has been a useful method to calculate cumulative genomic risk in health, which can explain a modest amount of depression risk and cognitive impairment [9, 10]. Effective connectivity of stress-related working memory information transfer across brain networks observed in the task has been reported to be influenced by $PM_{2.5}$ exposure to differing extents depending on the polygenic risk for depression [11]. Resting-state functional connectivity measuring correlations between low-frequency blood oxygen level-dependent (BOLD) fluctuations can identify "intrinsic" (i.e., task-independent) networks in the brain, which tend to be more stable across time than task-related activations. Although resting-state functional magnetic resonance imaging (rs-fMRI) studies examining intrinsic brain networks reported cortical thinning in regions of the default mode network (DMN) [12], local atrophy in the frontoparietal network [13], and reduced segregation of functional brain networks [14] associated with air pollution exposure, the interactive effect of genetic susceptibility and air pollution haven't been explored.

Air pollution may activate or inhibit the expression of genes [11] by DNA methylation (DNAm), an important epigenetic modification evidenced by the paradigm of DNAm changes [15], thereby translating the influences into phenotypic variations and affecting the function of the nervous system. Imaging-transcriptomic associations and DNAm analysis of whole blood cells can map gene expression profiles with neuroimaging phenotypes and explore the underlying biological mechanism. The investigation of gene-environment interactions can provide valuable insights into the neurobiological foundations and deleterious consequences of air pollution on the brain's association with cognition outcomes [16].

In the present study, we focused on the potential interactive effect of air pollution and genetic risk for depression on cognition, utilizing a cross-sectional research design to explore the underlying neural correlates. We hypothesized that air pollution increased the risk of cognitive impairment in people with a high genetic predisposition to depression by altering resting-state brain function via DNA methylation. First, we examined the associations between air pollution, genetic risk of MDD, and cognitive performance. Then, we elucidated the impact of recent air pollution exposure on resting-state brain function concerning polygenic risk for MDD across multiple levels of brain function—specifically, local intrinsic connectivity and global functional connectivity. Finally, we explored the potential underlying DNA methylation mechanism, focusing on depression-related genes that spatial co-expression patterns that align with local intrinsic connectivity, as identified through the unique Allen Brain Atlas resource, which provides densely sampled genome-wide expression data across multiple brain regions (Fig. 1). To our knowledge, this is the first study to examine $PM_{2.5}$-by-PRS interactive effect on

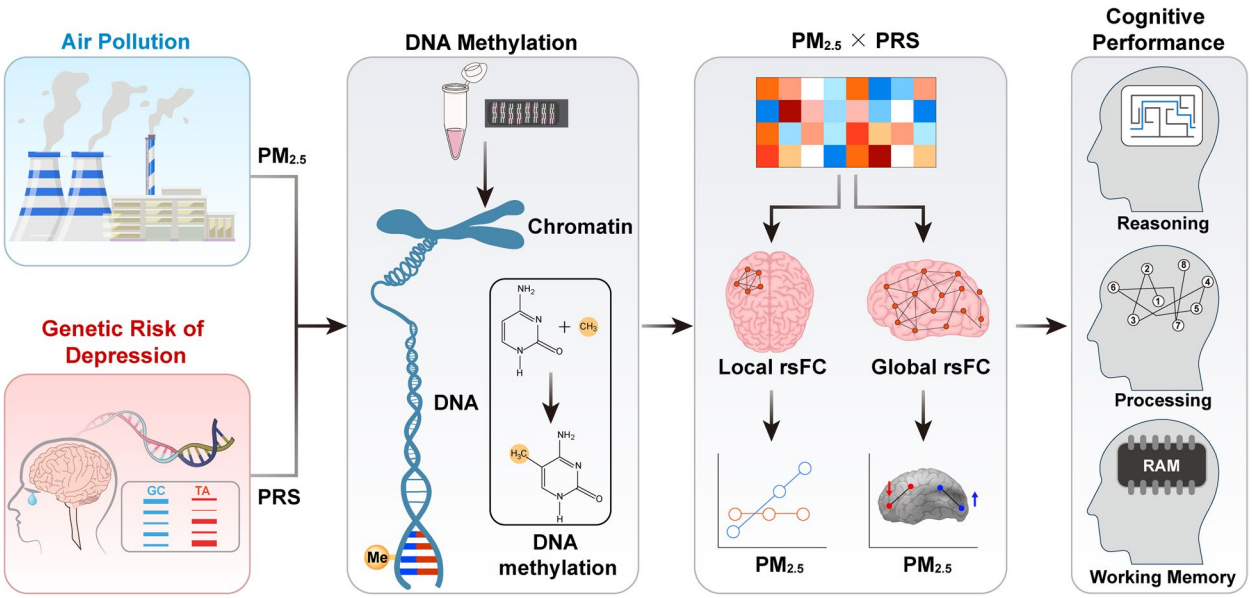

Fig. 1 Study overview. We hypothesized that air pollution increased the risk of cognitive impairment in people with a high genetic predisposition to depression by altering resting-state brain function (regional activity and brain network) via DNA methylation. The gene-environment interactive effect can be evaluated via a multiplicative interaction term between the air pollutant and the polygenic risk score (PRS) of depression to evaluate how air pollutants modified the effect of genetic susceptibility on brain function and cognition. First, we examined the effect of air pollution and genetic risk of depression on cognitive performance. Then, we elucidated the impact of recent air pollution exposure on resting-state brain function concerning polygenic risk for MDD across multiple levels of brain function, that is, regional activity and brain network. Finally, the underlying DNA methylation mechanism was explored. $PM_{2.5}$, particulate matter less than 2.5 μm; rsFC, resting-state functional connectivity

cognition and resting-state brain function, aiming to provide a more comprehensive understanding of the mechanisms involved.

Methods

Participants

We included 522 healthy participants living in Beijing in the present study from the local community from January 2014 to July 2016. Cognitive function was assessed using the Chinese version of MATRICS Consensus Cognitive Battery (MCCB) [17] including nine tests that evaluated seven domains of cognition including speed of processing, attention/vigilance, working memory, verbal learning, visual learning, reasoning and problem-solving, and social cognition. The raw MCCB scores were then converted to *T* scores based on comparing the individual's raw scores with those of a normative sample (of 656 individuals from six locations around China) [18] with a mean of 50 and a standard deviation of 10 (Additional File 1:Supplementary Methods and Table S1). This study was approved by the institutional ethics review board of Peking University Sixth Hospital. Written informed consent was obtained from all participants according to the Declaration of Helsinki.

Ambient air pollution estimates

We estimated each subject's air pollution exposure in the 6 months immediately before study participation based on public data published by the Ministry of Ecology and Environment of the People's Republic of China (https://www.mee.gov.cn/hjzl/) using average data from twelve air monitoring stations in Beijing (see stations information in Additional File 1: Supplementary Table S2). Considering all the participants lived in Beijing during the last 12 months, we estimated each subject's $PM_{2.5}$ exposure in the 6 months immediately prior to participation. The daily average data was calculated from hourly data from monitoring stations, and the monthly average data was generated from the daily average data from January 2014 to July 2016.

Resting-state fMRI processing

All participants were scanned on a 3.0 T GE scanner (Discovery MR750) at the Center for Neuroimaging, Peking University. Data preprocessing of resting-state fMRI was completed using DPABI [19]. The detailed parameters and preprocessing were described in Additional File 1: Supplementary Methods.

Local functional connectivity

Regional homogeneity (ReHo) is a measure of local functional brain connectivity that has demonstrated relevance in various neuropsychiatric disorders [20–22]. It assesses the functional connectivity relationships between a given node and its nearest neighboring nodes, essentially quantifying the degree of connections within local brain regions. After quantifying head motion by computing the volume-based framewise displacement (FD) [23], 497 patients were entered into the further imaging analysis. Resting-state fMRI data second-level analyses were conducted using SPM12 (Wellcome Department of Cognitive Neurology, London, UK). General linear models were applied to individual ReHo maps as the independent variables and PRS-by-$PM_{2.5}$ interactive effect as the dependent variable, and ReHo values were extracted. The significance threshold was set at a voxel level of $P<0.001$ uncorrected and a cluster level of $P<0.05$ with family-wise error (FWE) correction applied.

Global functional connectivity

The Brainnetome atlas, a map with more fine-grained functional brain subregions and detailed anatomical and functional connection patterns for each area containing 246 subregions of the bilateral hemispheres [24] (http://atlas.brainnetome.org/), was chosen to construct the individual global functional connectivity network. The time series of each region of interest (ROI) was extracted by averaging the time series of all voxels within it, and then we computed the Pearson correlation coefficient across subjects between the time signals of every pair of ROIs as the resting-state functional connectivity (rsFC), resulting in 30,135 ($246\times245/2$) links.

Partial least square regression (PLSR) was used as a dimensionality reduction strategy in Matlab R2020a to define orthogonal rsFC, in which this rsFC was influenced by the interaction of $PM_{2.5}$ exposure and polygenic risk for MDD. The gene-environment (G×E) interactions were evaluated via a multiplicative interaction term between $PM_{2.5}$ exposure and PRS. We set X to be a matrix of a functional network with each row representing a participant and each column representing a link, which was rsFC between two brain regions. We set Y to be a column vector of the G×E effect. PLSR searches for latent components that maximize the covariance between X and Y by performing a double decomposition of X and Y using singular value decomposition. In this way, PLSR seeks to find a set of orthogonal latent components of X that predict Y as accurately as possible. PLSR fits regression coefficients for each latent component to predict Y using multiple linear regression. By mapping these regression coefficients back to each functional connectivity, we generated one regression weight for each rsFC, whose absolute value quantifies its contribution to the prediction.

Polygenic risk score calculation

DNA was extracted by using the QIAamp DNA Mini Kit from whole blood samples and genotyped with the standard genotyping protocol on Illumina Human OmniZhongHua-8 Bead Chips. Details of the genotype quality control were described in the Supplemental Methods. The PRS of MDD were calculated from the imputed genotype dosage scores using large-scale GWAS summary statistics (as described in Additional File 1: Supplementary Table S3 [25, 26]) with a significant level of $P<5\times10^{-8}$ for both the European [25] and East Asian population [26] by PRSice-2 [27].

Imaging-transcriptome association

From the previous study [28], 39 genes showed differential gene expression in the precuneus than other brain regions (a log-fold change > 2 and a false discovery rate < 0.05). To identify similar gene candidates in our study, we conducted the imaging-transcriptome association analysis using PLSR in participants with a higher MDD risk ($N=74$, Fig. 3A). The Allen Human Brain Atlas (AHBA, http://human.brain-map.org), a publicly available whole-brain transcriptome dataset, was utilized to obtain gene expression data (Additional File 1: Supplementary Methods [29]). To elucidate the spatial distribution of transcriptional architecture in human cortical regions that corresponded to the ReHo map, potentially influenced by the interactive effect, PLSR analysis was performed in individuals with a high risk of MDD. The transcriptional matrix with each row representing a sample and each column representing the expression of each gene served as the predictor, and the mean ReHo *t*-value representing the G×E interactions was used as the response. The statistical significance of variance explained by the components was evaluated through 10,000 permutations. The component weights were normalized to *z*-scores based on standard errors obtained from 10,000 bootstrap replications, and false discovery rate (FDR) correction was applied.

DNA methylation

Peripheral blood samples from a subgroup of participants were selected to detect the DNA methylation profile. After matching for the length of time participants had lived in the urban, which might lead to differences in long-term air pollution, 280 healthy participants (Additional File 1: Supplementary Table S4) were subjected to genome-wide methylation profiling using the Illumina Infinium Human Methylation EPIC Beadchip, covering over 850,000 CpG sites. Following quality control

(Additional File 1: Supplementary Methods [30–32]), technical differences between two different probe types were normalized by beta-mixture quantile normalization method (BMIQ) [31] as implemented in the ChAMP R package [32]. Function champ.runCombat from ChAMP R package was used to conduct the correction of batch effect, and cell proportion was estimated by DNA Methylation Age Calculator. After normalization and correction for batch and cell type, 275 samples with 800,587 DNAm probes remained, as previously described [33]. We speculated that the significant gene expressions were partly affected by air pollution-induced DNAm. An approximate multi-component MLM-based association excluding the target was utilized to explore the association between DNAm probes and brain activities that showed G×E interactions.

Results

Demographic information and cognitive performance

A total of 497 healthy participants, with a median age of 24.0 years and educational attainment of 17.0 years, were included in the study. The median of $PM_{2.5}$ exposure in the 6 months preceding the study was 79.00 μg/m^3 (Table 1). The $PM_{2.5}$ exposure was negatively associated with reasoning and problem-solving performance ($r=-0.148$, $P=0.0011$, $P<0.05$ with Bonferroni correction across seven cognitive domains of the MCCB), processing speed ($r=-0.126$, $P=0.0055$, $P_{\text{Bonferroni}}<0.05$), and composite score ($r=-0.137$, $P=0.0025$, $P_{\text{Bonferroni}}<0.05$). When divided the sample into participants with a higher $PM_{2.5}$ exposure (higher than average, $n=305$) and a lower $PM_{2.5}$ exposure (lower than average, $n=192$), participants with a higher exposure showed worse processing speed ($F=11.146$, $P=0.0009$, effect size $f=0.150$), worse reasoning and problem-solving ($F=9.153$, $P=0.0026$, effect size $f=0.135$), and lower composite score ($F=15.397$, $P=0.0001$, effect size $f=0.176$).

Table 1 Demographics and cognitive performance of participants ($n=497$), *MCCB*, MATRICS Consensus Cognitive Battery

	Median (P25, P75)
Characteristics	
Age (years)	24.0 (22.0, 26.0)
Education (years)	17.0 (15.0, 19.0)
Gender (no. male/female)	242/255
$PM_{2.5}$ exposure (μg/m^3)	79.00 (68.17, 84.50)
MCCB	
Attention/vigilance	52.00 (46.00, 57.00)
Working memory	57.00 (51.00, 61.00)
Verbal learning	53.00 (48.00, 59.00)
Visual learning	59.00 (55.00, 62.00)
Reasoning and problem solving	50.00 (43.00, 58.00)
Social cognition	41.00 (34.00, 45.00)
Speed of processing	57.00 (52.00, 63.00)
Composite	53.14 (49.21, 55.86)

Furthermore, participants with a higher genetic risk (PRS higher than the average) were more likely to show worse processing speed when exposed to high levels of air pollution (beta = −1.34, $P=0.0197$, $n=240$) but not participants with a lower genetic risk (beta = −0.87, $P=0.090$, $n=257$) by using hierarchical regression with age, gender, and educational attainment as covariates. The PRS of MDD can account for up to 5% of the variance in processing speed (beta = −1.11, se = 0.42, $P=0.0078$).

Resting-state local and global functional connectivity

Interaction between PM2.5 exposure and polygenic risk of MDD on local functional connectivity

We uncovered a negative association between ReHo in the right precuneus gyrus and the interaction between $PM_{2.5}$ exposure and PRS of the European population (peak at [3 −63 57], $t=5.05$, $P_{\text{peak-level FWE}}=0.021$, cluster size = 56 voxels, $P_{\text{cluster-level FWE}}=0.028$, Fig. 2A). As $PM_{2.5}$ exposure increased, participants with higher PRS showed a decrease in ReHo of precuneus, while those with lower PRS exhibited an increase in ReHo (Fig. 2B).

Interaction between PM2.5 Exposure and polygenic risk of MDD on global functional connectivity

The top four PLSR components explained 57.18% of the variance in the G×E interaction effect, with the first component, PLSR-1, making a significant contribution to the interaction between $PM_{2.5}$ exposure and polygenic risk of MDD (21.04% explanation, $P=0.036$ with nonparametric permutation test, Additional File 1: Supplementary Fig. S1). PLSR-1 component was significantly positively associated with the interaction term of $PM_{2.5}$ exposure and polygenic risk for MDD (Fig. 2C, r = 0.458, $P<0.001$). The engagement of brain networks in PLSR-1 was disproportionately accentuated by $PM_{2.5}$ exposure in those with higher polygenic risk for MDD (Fig. 2D). While significant in the entire sample, this interaction is shown in a subset of individuals with relatively higher polygenic risk for depression (> mean + SD, $n=74$) and a subset of individuals with relatively lower polygenic risk (< mean − SD, $n=83$).

Among the 46 rsFC connections with |Z|-weighted loading > 5 and $P_{FDR}<0.05$ (Additional File 2: Supplementary Table S5), 8 of them had positive weight, while 38 had negative weight, representing a negative correlation with PRS-by-$PM_{2.5}$. Weaker functional connectivity patterns centered on the ventromedial prefrontal cortex

(vmPFC) were the primary contributors (showing top negative weights) to explaining gene-by-environment interactions, involving intra-orbitofrontal rsFC, frontal-parietal (vmPFC-precuneus), and frontal-limbic rsFCs (vmPFC-dACC) (Fig. 2E). Notably, one of the top 5 connections with a negative weight (Z = −5.46) was between the left precuneus and left vmPFC.

Correlation between functional connectivity and cognitive performance

The top two rsFCs that showed positive or negative weights (as described in Additional File 2: Supplementary Table S5) were selected as independent variables in the correlation analysis. The processing speed performances that showed the most significant between-group difference were chosen as the dependent variable. In the group with relatively higher (> mean + SD) PRS-MDD, the rsFC between left AG and left rostral cuneus gyrus, which increased with greater $PM_{2.5}$ exposure (Fig. 2F) was marginally negatively correlated with processing speed score after applying the Bonferroni correction (beta = −9.38, $P = 0.014$, $P_{\text{Bonferroni}} = 0.058$, $n = 74$, Fig. 2G) with age, gender, and educational attainment as covariates. The causal mediation analysis showed that the relationship between air pollution exposure and processing speed was partly mediated by this rsFC ($\beta = -0.0537$, $P = 0.041$, 95%CI [−0.1334, −0.00143], Additional File 1: Supplementary Fig. S2 [34]).

Gene expression and DNA methylation

Region-specific expression and imaging-transcriptome association

We found that the top four PLSR components accounted for 17.81% of the variance in gene-environment interaction in ReHo (Additional File 2: Supplementary Table S6). Notably, PLS1 consisted of 315 significant genes enriched in the process of vesicle-mediated transport in the synapse, cell types of glutamatergic synapse and microglia cells, and interactive with interleukin 6 (IL-6) (Fig. 3B, C).

DNA methylation

Among these 315 significant genes, we found that 14 genes exhibited a positive weight consistent with the previously reported overexpression pattern and overlapped with the 39 genes displaying differential gene expression. We identified a total of 90 DNAm probes located in CpG islands within the 14 genes of interest. For statistical significance, we set the threshold at $P < 5.56 \times 10^{-4}$ (0.05/90), and a suggestive threshold at $P < 5 \times 10^{-3}$. Interestingly, we observed a suggestive negative association with one specific CpG island, cg18219563, located in the promoter region of the Solute Carrier Family 30 Member 3 (*SLC30A3*) gene ($P = 0.004$, Fig. 3A). Moreover, the methylation levels of cg18219563 in the prefrontal cortex showed a significant correlation with those in the peripheral blood ($r = 0.231$, $P = 0.0474$, $n = 74$, Additional File 1: Supplementary Fig. S3). The expression quantitative-trait loci for the *SLC30A3* gene affects the expression in a wide

(See figure on next page.)

Fig. 2 Interaction between $PM_{2.5}$ Exposure and polygenic risk of MDD on resting-state brain connectivity. **A** The regional homogeneity (ReHo) in the right precuneus gyrus was negatively associated with the interaction between $PM_{2.5}$ exposure and PRS-MDD (peak at [3 −63 57], $t = 4.99$, cluster size = 56 voxels, $P_{\text{cluster-level FWE}} = 0.024$). The color bar indicates the *t*-value of generalized linear analysis. **B** With increasing $PM_{2.5}$ exposure, participants with higher PRS-MDD (high PRS) showed decreased ReHo in the precuneus, while those with lower PRS-MDD (low PRS) showed increased ReHo. **C** Correlation between the partial least square regression (PLSR) component scores and the interaction term of $PM_{2.5}$ exposure and polygenic risk for MDD ($n = 497$). The PLSR-1 component explained the largest variance and showed a significant gene-by-environment interaction. The engagement of brain networks in PLSR-1 was disproportionately accentuated by $PM_{2.5}$ exposure in those with higher polygenic risk for MDD. While significant in the entire sample, this interaction is shown in a subset of individuals with relatively higher polygenic risk for depression (red, > mean + SD, $n = 74$) and a subset of individuals with relatively lower polygenic risk (blue, < mean − SD, $n = 83$). **D** The engagement of brain networks in PLSR-1 was disproportionately accentuated by $PM_{2.5}$ exposure in those with higher polygenic risk for MDD. While significant in the entire sample, this interaction is shown in a subset of individuals with relatively higher polygenic risk for depression (red, > mean + SD, $n = 74$) and a subset of individuals with relatively lower polygenic risk (blue, < mean − SD, $n = 83$). **E** Partial least square regression analysis revealed 46 rsFC survived with a significant correlation with the gene-by-environment interaction between polygenic risk of MDD and $PM_{2.5}$ Exposure (8 rsFC with loading $Z > 0$, 38 rsFC with loading $Z < 0$). The outermost circle represents the name of the brain lobes, and the second circle represents the brain regions within the lobes with the same color. Red lines represent rsFC with positive loadings, and blue lines represent rsFC with negative loadings. For the full names corresponding to the abbreviations of the brain regions in the innermost circle, see Supplementary Table S5. **F** The correlation between $PM_{2.5}$ and left angular gyrus (AG)—left cuneus (CUN) resting-state functional connectivity was plotted in a subsample of individuals with relatively higher polygenic risk of depression (PRS > mean + SD and $n = 74$, red), compared to those with relatively lower polygenic risk (PRS < mean − SD and $n = 82$, blue). **G** The correlation between left angular gyrus (AG)—left cuneus (CUN) resting-state functional connectivity and processing speed was plotted in a subsample of individuals with relatively higher polygenic risk of depression (PRS > mean + SD and $n = 74$, red), compared to those with relatively lower polygenic risk (PRS < mean − SD and $n = 82$, blue). $PM_{2.5}$, particulate matter less than 2.5 μm; PRS-by-PM2.5 interaction effect, interactive effect of air pollution and genetic risk of depression; MDD, major depressive disorder; PRS, polygenic risk score of MDD

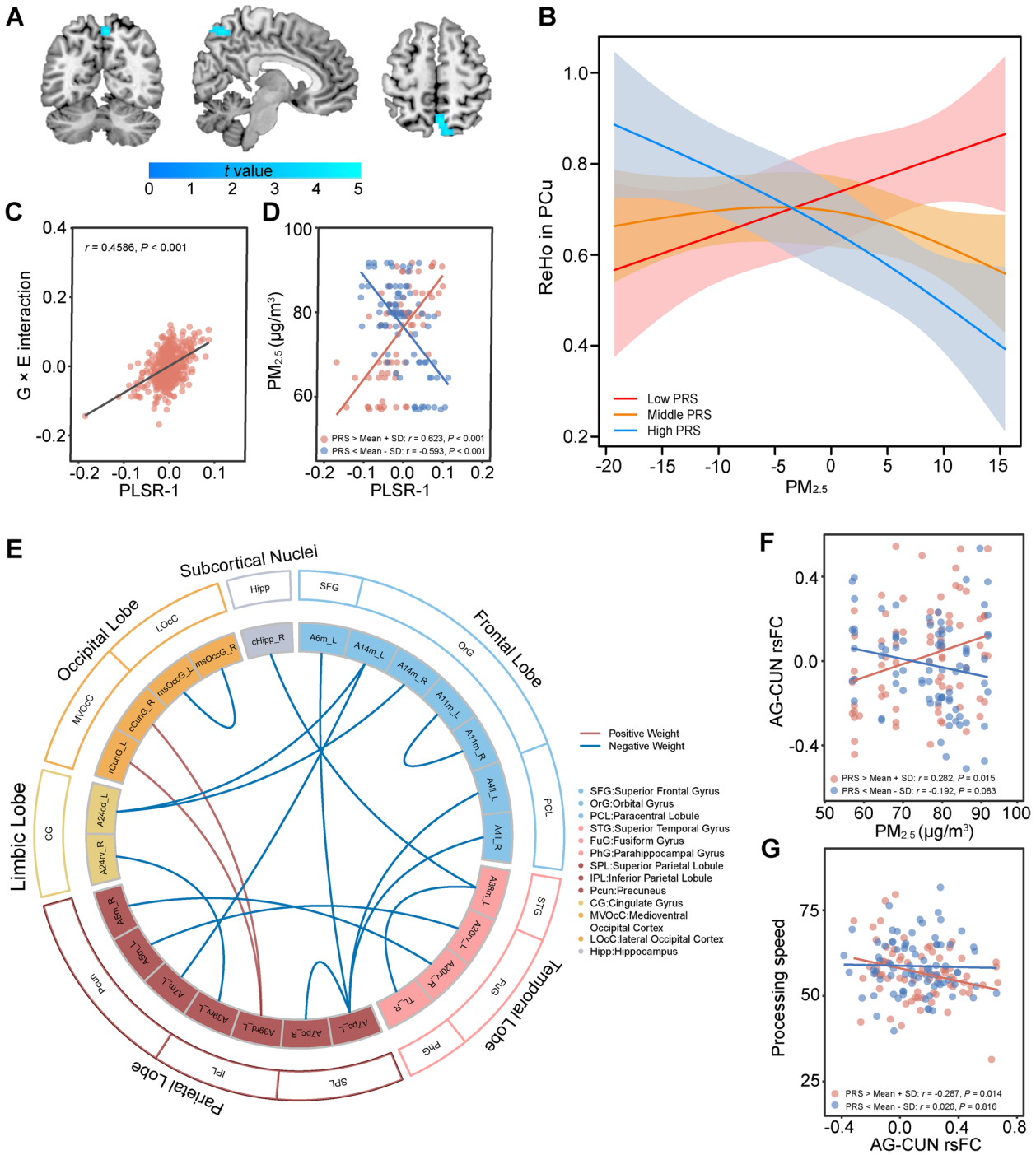

Fig. 2 (See legend on previous page.)

range of brain regions, especially the prefrontal cortex [36] (Additional File 1: Supplementary Fig. S4).

Discussion

In our study, local spontaneous activity in precuneus was influenced by $PM_{2.5}$ exposure to differing polygenic risk for depression. Weaker functional connectivity patterns centralized of vmPFC partly accounted for the gene-by-environment interactions. Increased FC between AG and cuneus gyrus was associated with this interactive effect, and negatively correlated with processing speed. The local activity in precuneus of individuals with a higher polygenic risk for depression showed a correlation with gene expression and DNA methylation of *SLC30A3*,

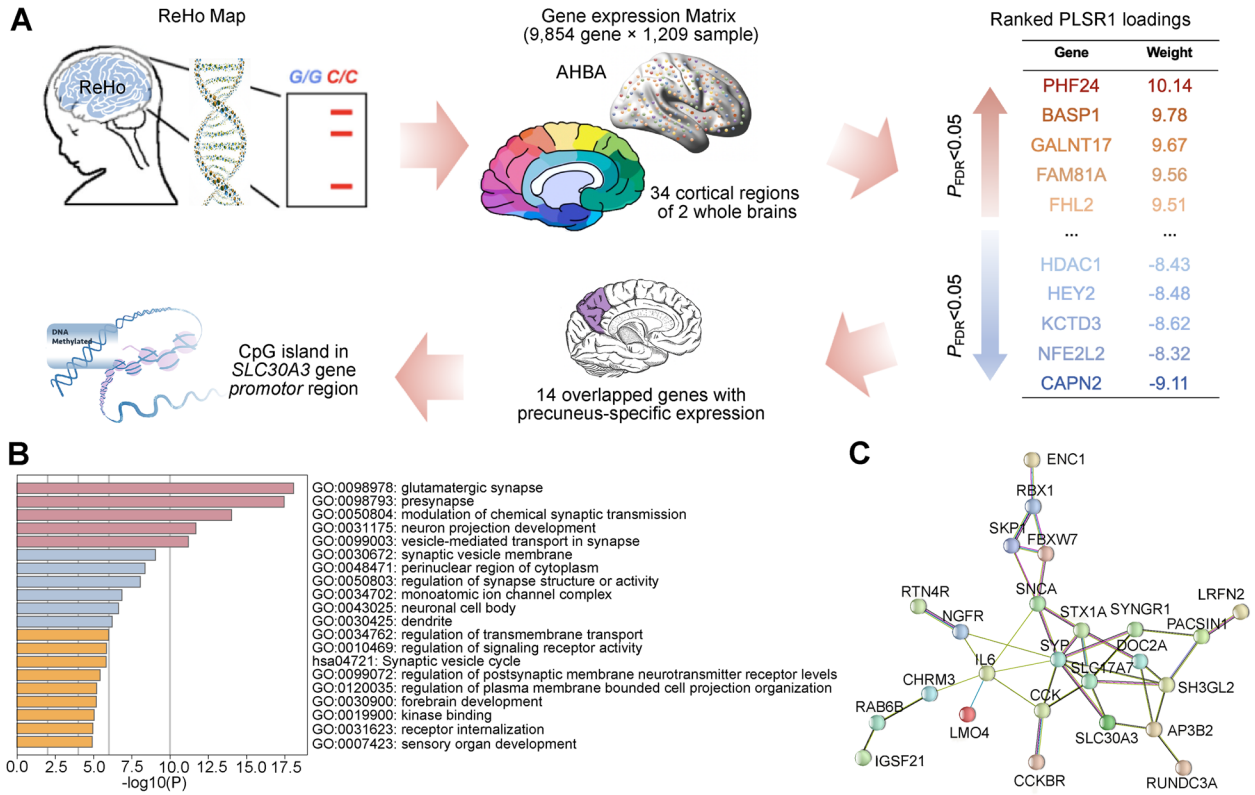

Fig. 3 Gene expression profiles and DNA methylation analyses. **A** ReHo associated with the interaction between $PM_{2.5}$ exposure and PRS-MDD in the individuals with higher MDD genetic risk was parcellated into the Desikan-Killiany (DK) atlas and the overlapped 1209 samples with averaged gene expressions were obtained from Allen Human Brain Atlas in cortical regions across two postmortem brains. After generating the gene expression matrix, partial least squares (PLS) regression was used to identify imaging-transcriptomic associations, and the regional first PLSR component (PLS1) scores (a weighted sum of 9854 gene expression scores) and regional changes were observed ($r_{Pearson} = 0.254$). The ranked PLS1 loadings were shown with gene names and weights|. After overlapping with genes that showed precuneus-specific expression, DNA methylation probes located in CpG island in 14 genes were inputted to test the association between the probes and ReHo showing gene-by-environment interaction. CpG island cg18219563 in the *SLC30A3* gene promotor region showed a suggestive negative association ($P = 0.0040$). **B** Enrichment of biological processes of genes showing significant spatial expressions. The gene ontology (GO) biological processes were aligned with the overlapped gene list using Metascape [35] (https://metascape.org) and corrected by FDR with $P < 0.05$. **C** Protein products interaction of genes showing significant spatial expressions plus interleukin 6. The top 50 genes with the positive weight of PLS1 genes using PLSR in participants with a higher MDD risk plus interleukin 6 were entered into protein–protein interactions analysis. Edge colors represent different evidence underlying predicted protein–protein interactions in the STRING database. Images within spheres represent known protein structures; node color is aesthetic

known to be involved in oxidative stress and cognition. Air pollution might heighten the likelihood of cognitive impairment in individuals genetically predisposed to depression by modifying the resting-state brain function through DNA methylation.

Experimental studies support the hypothesis that $PM_{2.5}$ acts as a developmental neurotoxicant [37, 38]. The neuronal activation and damage caused by air pollution included direct inflammation via particles and toxins crossing blood–brain barrier (BBB). In $PM_{2.5}$-polluted human brain models established on a 3D microfluidic platform, the penetration of $PM_{2.5}$ across the BBB which triggers astrogliosis resulting in neuronal loss and microglial infiltration has been validated [39]. Internal and external factors contribute to individual cognitive responses to air pollutants [40]. Dysregulation of the precuneus, which plays a role in cognitive control processes (e.g., self-processing, spatial imagery, episodic memory retrieval) has been associated with depression, which is correlated with low self-esteem [41]. Studies on MDD patients have shown decreased network homogeneity [42] and impaired spontaneous neural activity in the precuneus measured by ReHo [43, 44]. Our observed decrease in precuneus ReHo in participants with higher MDD risk, coupled with increased $PM_{2.5}$ exposure, was in line with these existing findings.

VmPFC plays a critical role in generating and regulating negative emotions, interacting with the amygdala, hippocampus, and dorsal anterior cingulate cortex (dACC) [45]. In our study, weaker functional connectivity

patterns centered on the vmPFC were the primary contributors to explaining gene-by-environment interactions, involving intra-orbitofrontal rsFC, frontal-parietal (vmPFC-precuneus), and frontal-limbic FCs (vmPFC-dACC). Both the precuneus and vmPFC serve as key hubs of DMN [46]. VmPFC has been shown to modulate threat and reward responses in the common marmoset [47]. Changes in regional activation in the vmPFC and precuneus reflected trait markers of depression related to neural responses to psychosocial stress [48]. Reward sensitivity in healthy adults [49] and treatment response in MDD patients [50] were associated with rsFC between vmPFC and ACC. The weaker functional connectivity between regions belonging to the DMN (i.e., between the vmPFC and the precuneus, intra-orbitofrontal rsFC), might indicate lower intra-network integration [51], while the weaker functional connectivity between the vmPFC and dACC indicated lower collaboration of the affective-cognitive network [52].

The occipitoparietal network plays a crucial role in visually guided action, somatosensation, spatial audition, navigation, and spatial working memory [53]. The cuneus and angular gyrus (AG) were both involved in visual circuit. The cuneus is necessary for both basic and higher-level visual processing and acts to modulate signals traveling from the primary visual cortex to the extrastriate cortices [54]. AG affected decision-making requiring visuospatial attention [55] and involved in the retrieval of both episodic and semantic information and subjective experience of remembering [56]. In our study, exposing more pollution, individuals with higher MDD risk showed increased rsFC negatively correlated with processing speed, which indicated a loss of flexibility in information processing [57]. This may be related to functional changes in the precuneus and angular gyrus, as these two brain regions play key roles in both visual information processing and spatial working memory. Further studies have also found that the occipitoparietal network can be enhanced by transcranial alternating current stimulation (tACS) that mimics endogenous attentional states [58]. This network modulation was able to increase the variability of single-trial psychometric thresholds, as evidenced by reduced reaction times. This suggests that the occipitoparietal network not only plays an important role in the encoding and processing of visual information, but also plays a key role in improving the precision and efficiency of visually guided movements.

DNA methylation, as a crucial epigenetic modification, plays a pivotal role in regulating gene expression and is highly susceptible to environmental factors. The negative association between ReHo in the precuneus and gene-environment interaction was suggestively linked to *SLC30A3* methylation. *SLC30A3*, also known as *ZnT3*, encodes a zinc transporter-3 protein responsible for maintaining zinc-glutamate homeostasis at the glutamatergic synapse. Research has identified zinc metabolism as a potential therapeutic target for depression [59], with *ZnT3* knock-out mice exhibiting synaptic and memory deficits [60]. Insufficient vesicular zinc has been shown to alter the behavioral effects of social defeat stress [61]. A decrease in ZnT3 protein was found in PFC of MDD and associated with suicide [62]. Zinc is an essential nutrient vital for human health possessing antioxidative stress properties [63], and could reduce IL-6 levels and memory deficit in mice [64]. Oxidative stress, a common feature underlying the harmful effects of air pollutants, can generate reactive oxygen/nitrogen species [65]. Post-mortem examinations of individuals with high exposure to air pollution have revealed elevated levels of oxidative stress indicators and neuroinflammation [66]. The penetration of $PM_{2.5}$ across BBB and its accumulation in brain tissue by additional proinflammatory mediators and nitric oxide have been validated [39]. Although the correlation was suggestive and needed to be interpreted carefully, the identified correlation between hypermethylation of the *SLC30A3* gene and local spontaneous activity in the precuneus raises the possible link between zinc-associated oxidative stress, neuroinflammation, and brain activity to the impact of air pollution in higher MDD genetic risk individuals.

Lifestyle modifications (e.g., minimize outdoor activities and do indoor moderate physical activity during times of high air pollution concentrations) and environmental exposure reduction (e.g., wearing a mask on high pollution days) could be beneficial in mitigating the impact of air pollution on individuals with high genetic susceptibility to depression. Our results also possibly informed the development of screening methods for susceptibility to environmental risks by combining genetic and environmental risks or recognizing rsFC changes. However, it is important to consider the limitations of our study. Firstly, significant G × E interactions were only observed when using PRS calculated from the European population. Future studies could employ bioinformatic advancements that account for ancestry differences. Secondly, DNA methylation of the *SLC30A3* gene was suggestively associated with the local spontaneous activity in precuneus, which was conducted within 14 candidate genes and needed to be verified in an independent sample. Thirdly, our approach for estimating air pollution exposure relies on residential addresses and historical data. Although we selected the addresses where individuals resided for the longest duration during the past 6 months, this method could still result in discrepancies due to indoor pollution sources and is less precise compared to Land-use models or other advanced methods. Furthermore, our

investigation focused on recent air pollution exposures over a 6-month period in adults, a length of time that could affect the risk for cognition [67]. The long-term cumulative effects and air pollution exposure during important or sensitive neurodevelopment periods (e.g., prepartum, childhood) might well yield additional disease mechanisms, which could be further investigated. Last, to minimize the influence of potential confounders and control the quality of image data, we used a strict exclusion criterion, potentially limiting the generalizability of the findings.

Conclusions

In summary, our cross-sectional study suggests that the polygenic risk for MDD may be associated with an enhanced neural impact of $PM_{2.5}$ exposure, particularly affecting the precuneus and weakening the rsFC of the occipitoparietal network correlated with processing speed. These findings underscore the potential intricate relationships among genetic factors, environmental influences, brain functioning, and cognition.

Abbreviations

AG	Angular gyrus
AHBA	Allen Human Brain Atlas
BBB	Blood-brain barrier
BOLD	Blood oxygen level-dependent
BMIQ	Beta-mixture quantile normalization method
dACC	Dorsal anterior cingulate cortex
DMN	Default mode network
DNAm	DNA methylation
FD	Framewise displacement
FDR	False discovery rate
fMRI	Functional magnetic resonance imaging
FWE	Family-wise error
G×E	Gene-environment interactions
IL-6	Interleukin 6
MCCB	MATRICS Consensus Cognitive Battery
MDD	Major depressive disorder
$PM_{2.5}$	Fine particulate matter with a diameter of less than or equal to 2.5 μm
PLSR	Partial least squares regression
PRS	Polygenic risk score
PRS-by-$PM_{2.5}$	Interaction between polygenic risk score and $PM_{2.5}$
ReHo	Regional homogeneity
ROI	Region of interest
rs-fMRI	Resting-state functional magnetic resonance imaging
rsFC	Resting-state functional connectivity
SLC30A3	Solute carrier family 30 member 3
tACS	Transcranial alternating current stimulation
vmPFC	Ventromedial prefrontal cortex

Supplementary Information

The online version contains supplementary material available at https://doi.org/10.1186/s12916-024-03614-6.

Supplementary Material 1. Supplementary Methods. Table S1-S4, Figure S1-S4. Table S1. Cognitive domains and description of the cognitive tests. Table S2. Information of Monitoring stations in Beijing used to estimate PM<Subscript>2.5</Subscript> exposure. Table S3. GWAS summary statistics for polygenic risk score calculation. Table S4. Comparison of demographics and cognitive performance of participants in two groups. Figure S1. Percent variance explained in gene-environment interaction of rsFC. Figure S2. Causal mediation model in participants with a higher genetic risk of depression. Figure S3. The Blood Brain DNA Methylation Comparison of cg18219563. Figure S4. Overview of eQTL for SLC30A3 (± 10M region) from QTLbase database.

Supplementary Material 2. Table S5-S6. Table S5. PLSR1 resting-state functional connectivity that significantly spatially correlated with gene-environment interaction. Table S6. PLSR1 genes that significantly spatially correlated with gene-environment interaction in ReHo in participants with higher depression risk.

Acknowledgements

We extend our gratitude to all subjects who participated in this study. We thank the Allen Institute for Brain Science founders and staff who supplied the brain expression data.

Y.Z.: conceptualization, data curation, formal analysis, funding acquisition, investigation, methodology, visualization, writing the original draft, revision, and discussion of the final edition. Y.S.: conceptualization, methodology. L.G.: methodology, visualization. X.Z., Y.L, Z.K., X.F., G.Z., J.S., Y.Y: methodology, interpretation. H.Y. and D.Z.: conceptualization, project administration. Z.L. and W.Y: conceptualization, supervision, methodology, funding acquisition, project administration, revision, and discussion of the final edition. All authors read and approved the final version of the manuscript.

Funding

This work was supported by the National Natural Science Foundation of China (82301687; 82330042), National Key R&D Program of China (2023YFE0119400; 2021YFF1201100); STI2030-Major Projects-2021ZD0200702; Capital's Funds for Health Improvement and Research (2024–1-4111); China Postdoctoral Science Foundation (2022M720302); National Postdoctoral Program for Innovative Talents (BX20240029); Academy of Medical Sciences Research Unit (2019-I2M-5–006); Fundamental Research Funds for the Central Universities (Peking University Medicine Fund for world's leading discipline or discipline cluster development, BMU2022DJXK007); Clinical Medicine Plus X—Young Scholars Project, Peking University, the Fundamental Research Funds for the Central Universities (PKU2023LCXQ028).

Availability of data and materials

The data that support the findings of this study are available from the corresponding author upon reasonable request.

Declarations

Ethics approval and consent to participate

This study was approved by the Ethics Committee of Peking University Sixth Hospital (2013–13) and Johns Hopkins University School of Medicine (NA_00088322). Written consent was obtained from each subject after the description of the study.

Consent for publication

Consent.

Competing interests

The authors declare that they have no known competing financial interests or personal relationships that could have appeared to influence the work reported in this paper.

Author details

[1]Peking University Sixth Hospital, Peking University Institute of Mental Health, NHC Key Laboratory of Mental Health (Peking University), National Clinical Research Center for Mental Disorders (Peking University Sixth Hospital), Beijing 100191, China. [2]Chinese Institute for Brain Research, Beijing 102206, China. [3]PKU-IDG/McGovern Institute for Brain Research, Peking University, Beijing 100871, China. [4]Research Unit of Diagnosis and Treatment of Mood Cognitive Disorder (2018RU006), Chinese Academy of Medical Sciences, Beijing 100191, China.

Received: 25 March 2024 Accepted: 4 September 2024
Published online: 13 September 2024

References

1. Vigo D, Thornicroft G, Atun R. Estimating the true global burden of mental illness. Lancet Psychiatry. 2016;3:171–8.
2. Qiu X, et al. Association of long-term exposure to air pollution with late-life depression in older adults in the US. JAMA Netw Open. 2023;6: e2253668.
3. Fu Z, et al. Air pollution, genetic factors and the risk of depression. Sci Total Environ. 2022;850: 158001.
4. Gao X, Jiang M, Huang N, Guo X, Huang T. Long-term air pollution, genetic susceptibility, and the risk of depression and anxiety: a prospective study in the UK Biobank cohort. Environ Health Perspect. 2023;131:17002.
5. Ehsanifar M, Montazeri Z, Zavareh MS, Rafati M, Wang J. Cognitive impairment, depressive-like behaviors and hippocampal microglia activation following exposure to air pollution nanoparticles. Environ Sci Pollut Res Int. 2023;30:23527–37.
6. Varghese S, Frey BN, Schneider MA, Kapczinski F, de Azevedo Cardoso T. Functional and cognitive impairment in the first episode of depression: a systematic review. Acta Psychiatr Scand. 2022;145:156–85.
7. Costa LG, Cole TB, Dao K, Chang YC, Garrick JM. Developmental impact of air pollution on brain function. Neurochem Int. 2019;131: 104580.
8. Zhu A, et al. Interaction between plant-based dietary pattern and air pollution on cognitive function: a prospective cohort analysis of Chinese older adults. Lancet Reg Health West Pac. 2022;20: 100372.
9. Mitchell BL, et al. Polygenic risk scores derived from varying definitions of depression and risk of depression. JAMA Psychiat. 2021;78:1152–60.
10. Xu J, et al. Neurobiological substrates underlying the effect of genomic risk for depression on the conversion of amnestic mild cognitive impairment. Brain. 2018;141:3457–71.
11. Li Z, et al. Air pollution interacts with genetic risk to influence cortical networks implicated in depression. Proc Natl Acad Sci U S A. 2021;118:e2109310118.
12. Lucht S, et al. Long-term air pollution, noise, and structural measures of the default mode network in the brain: results from the 1000BRAINS cohort. Int J Hyg Environ Health. 2022;239: 113867.
13. Nussbaum R, et al. Associations of air pollution and noise with local brain structure in a cohort of older adults. Environ Health Perspect. 2020;128:67012.
14. Glaubitz L, et al. Association between long-term air pollution, chronic traffic noise, and resting-state functional connectivity in the 1000BRAINS study. Environ Health Perspect. 2022;130:97007.
15. Martin EM, Fry RC. Environmental influences on the epigenome: exposure- associated DNA methylation in human populations. Annu Rev Public Health. 2018;39:309–33.
16. Essers E, et al. Air pollution exposure during pregnancy and childhood, APOE ε4 status and Alzheimer polygenic risk score, and brain structural morphology in preadolescents. Environ Res. 2023;216(Pt 2):114595.
17. Nuechterlein KH, et al. The MATRICS consensus cognitive battery, part 1: test selection, reliability, and validity. Am J Psychiatry. 2008;165:203–13.
18. Shi C, et al. The MATRICS Consensus Cognitive Battery (MCCB): co-norming and standardization in China. Schizophr Res. 2015;169:109–15.
19. Yan CG, Wang XD, Zuo XN, Zang YF. DPABI: data processing & analysis for (Resting-State) brain imaging. Neuroinformatics. 2016;14:339–51.
20. Adhikari BM, et al. Cerebral blood flow and cardiovascular risk effects on resting brain regional homogeneity. Neuroimage. 2022;262: 119555.
21. Cai M, et al. Disrupted local functional connectivity in schizophrenia: an updated and extended meta-analysis. Schizophrenia (Heidelb). 2022;8:93.
22. Xu X, et al. Effect of regional intrinsic activity following two kinds of theta burst stimulation on precuneus. Hum Brain Mapp. 2023;44:2254–65.
23. Jenkinson M, Bannister P, Brady M, Smith S. Improved optimization for the robust and accurate linear registration and motion correction of brain images. Neuroimage. 2002;17:825–41.
24. Fan LZ, et al. The human brainnetome atlas: a new brain atlas based on connectional architecture. Cereb Cortex. 2016;26:3508–26.
25. Howard DM, et al. Genome-wide meta-analysis of depression identifies 102 independent variants and highlights the importance of the prefrontal brain regions. Nat Neurosci. 2019;22:343–52.
26. Giannakopoulou O, et al. The genetic architecture of depression in individuals of east asian ancestry: a genome-wide association study. JAMA Psychiat. 2021;78:1258–69.
27. Choi SW, O'Reilly PF. PRSice-2: Polygenic risk score software for biobank-scale data. Gigascience. 2019;8:giz082.
28. Williams JA, et al. Inflammation and brain structure in Schizophrenia and other neuropsychiatric disorders: a mendelian randomization study. JAMA Psychiat. 2022;79:498–507.
29. Arnatkeviciute A, Fulcher BD, Fornito A. A practical guide to linking brain-wide gene expression and neuroimaging data. Neuroimage. 2019;189:353–67.
30. Nordlund J, et al. Genome-wide signatures of differential DNA methylation in pediatric acute lymphoblastic leukemia. Genome Biol. 2013;14: r105.
31. Zhou W, Laird PW, Shen H. Comprehensive characterization, annotation and innovative use of Infinium DNA methylation BeadChip probes. Nucleic Acids Res. 2017;45: e22.
32. Tian Y, et al. ChAMP: updated methylation analysis pipeline for Illumina BeadChips. Bioinformatics. 2017;33:3982–4.
33. Cheng W, Luo N, Zhang Y, Zhang X, Tan H, Zhang D, Sui J, Yue W, Yan H. DNA methylation and resting brain function mediate the association between childhood urbanicity and better speed of processing. Cereb Cortex. 2021;31:4709–18.
34. Zhonglin W, Baojuan Y. Analyses of mediating effects: the development of methods and models. Adv Psychol Sci. 2014;22:731–45.
35. Zhou Y, et al. Metascape provides a biologist-oriented resource for the analysis of systems-level datasets. Nat Commun. 2019;10:1523.
36. Wang D, et al. Comprehensive functional genomic resource and integrative model for the human brain. Science. 2018;362(6420):eaat8464.
37. Morris-Schaffer K, et al. Limited developmental neurotoxicity from neonatal inhalation exposure to diesel exhaust particles in C57BL/6 mice. Part Fibre Toxicol. 2019;16:1.
38. Wang Y, et al. Exposure to PM2.5 aggravates Parkinson's disease via inhibition of autophagy and mitophagy pathway. Toxicology. 2021;456: 152770.
39. Kang YJ, Tan HY, Lee CY, Cho H. An air particulate pollutant induces neuroinflammation and neurodegeneration in human brain models. Adv Sci (Weinh). 2021;8:e2101251.
40. Thompson R, et al. Air pollution and human cognition: A systematic review and meta-analysis. Sci Total Environ. 2023;859: 160234.
41. Cheng W, et al. Functional connectivity of the precuneus in unmedicated patients with depression. Biol Psychiatry Cogn Neurosci Neuroimaging. 2018;3:1040–9.
42. Luo L, et al. Decreased connectivity in precuneus of the ventral attentional network in first-episode, treatment-naive patients with major depressive disorder: a network homogeneity and independent component analysis. Front Psychiatry. 2022;13: 925253.
43. Zhong X, Pu W, Yao S. Functional alterations of fronto-limbic circuit and default mode network systems in first-episode, drug-naive patients with major depressive disorder: A meta-analysis of resting-state fMRI data. J Affect Disord. 2016;206:280–6.
44. Zhou M, et al. Intrinsic cerebral activity at resting state in adults with major depressive disorder: A meta-analysis. Prog Neuropsychopharmacol Biol Psychiatry. 2017;75:157–64.
45. Hiser J, Koenigs M. The multifaceted role of the ventromedial prefrontal cortex in emotion, decision making, social cognition, and psychopathology. Biol Psychiatry. 2018;83:638–47.
46. Buckner RL, DiNicola LM. The brain's default network: updated anatomy, physiology and evolving insights. Nat Rev Neurosci. 2019;20:593–608.
47. Stawicka ZM, et al. Ventromedial prefrontal area 14 provides opposing regulation of threat and reward-elicited responses in the common marmoset. Proc Natl Acad Sci U S A. 2020;117:25116–27.
48. Ming Q, et al. State-independent and dependent neural responses to psychosocial stress in current and remitted depression. Am J Psychiatry. 2017;174:971–9.
49. Adrian-Ventura J, Costumero V, Parcet MA, Avila C. Reward network connectivity "at rest" is associated with reward sensitivity in healthy adults: a resting-state fMRI study. Cogn Affect Behav Neurosci. 2019;19:726–36.
50. Kozel FA, et al. Functional connectivity of brain structures correlates with treatment outcome in major depressive disorder. Front Psychiatry. 2011;2: 7.
51. Pujol J, et al. Traffic pollution exposure is associated with altered brain connectivity in school children. Neuroimage. 2016;129:175–84.
52. Canu E, et al. Breakdown of the affective-cognitive network in functional dystonia. Hum Brain Mapp. 2020;41:3059–76.

53. Kravitz DJ, Saleem KS, Baker CI, Ungerleider LG, Mishkin M. The ventral visual pathway: an expanded neural framework for the processing of object quality. Trends Cogn Sci. 2013;17:26–49.
54. Vanni S, Tanskanen T, Seppa M, Uutela K, Hari R. Coinciding early activation of the human primary visual cortex and anteromedial cuneus. Proc Natl Acad Sci U S A. 2001;98:2776–80.
55. Studer B, Cen D, Walsh V. The angular gyrus and visuospatial attention in decision-making under risk. Neuroimage. 2014;103:75–80.
56. Bonnici HM, Richter FR, Yazar Y, Simons JS. Multimodal feature integration in the angular gyrus during episodic and semantic retrieval. J Neurosci. 2016;36:5462–71.
57. Uddin LQ. Cognitive and behavioural flexibility: neural mechanisms and clinical considerations. Nat Rev Neurosci. 2021;22:167–79.
58. Misselhorn J, Fiene M, Radecke JO, Engel AK, Schneider TR. Transcranial alternating current stimulation over frontal eye fields mimics attentional modulation of visual processing. J Neurosci. 2024;44:e1510232024.
59. Whitfield DR, et al. Depression and synaptic zinc regulation in Alzheimer disease, dementia with lewy bodies, and Parkinson disease dementia. Am J Geriatr Psychiatry. 2015;23:141–8.
60. Adlard PA, Parncutt JM, Finkelstein DI, Bush AI. Cognitive loss in zinc transporter-3 knock-out mice: a phenocopy for the synaptic and memory deficits of Alzheimer's disease? J Neurosci. 2010;30:1631–6.
61. McAllister BB, Wright DK, Wortman RC, Shultz SR, Dyck RH. Elimination of vesicular zinc alters the behavioural and neuroanatomical effects of social defeat stress in mice. Neurobiol Stress. 2018;9:199–213.
62. Rafalo-Ulinska A, et al. Zinc transporters protein level in postmortem brain of depressed subjects and suicide victims. J Psychiatr Res. 2016;83:220–9.
63. Choi S, Liu X, Pan Z. Zinc deficiency and cellular oxidative stress: prognostic implications in cardiovascular diseases. Acta Pharmacol Sin. 2018;39:1120–32.
64. de Oliveira S, et al. Zinc supplementation decreases obesity-related neuroinflammation and improves metabolic function and memory in rats. Obesity (Silver Spring). 2021;29:116–24.
65. Saenen ND, et al. Air pollution-induced placental alterations: an interplay of oxidative stress, epigenetics, and the aging phenotype? Clin Epigenetics. 2019;11:124.
66. Calderon-Garciduenas L, et al. Brain immune interactions and air pollution: macrophage inhibitory factor (MIF), prion cellular protein (PrP(C)), Interleukin-6 (IL-6), interleukin 1 receptor antagonist (IL-1Ra), and interleukin-2 (IL-2) in cerebrospinal fluid and MIF in serum differentiate urban children exposed to severe vs. low air pollution. Front Neurosci. 2013;7:183.
67. Zhang X, Chen X, Zhang X. The impact of exposure to air pollution on cognitive performance. Proc Natl Acad Sci U S A. 2018;115:9193–7.

Publisher's Note